An Approach for the BH Curve Identification of Magnetic Core of Synchronous Reluctance Machines

Abdolmajid Abedini Mohammadi[1,2], Adrian-Cornel Pop[1], Johan Gyselinck[2], *member, IEEE*

[1]BEAMS department, Université Libre de Bruxelles, Brussels, Belgium

[2]Drives/Simulation Group, Brose Fahrzeugteile SE & Co. KG, Würzburg, Germany

A method for BH curve identification of the magnetic core of synchronous reluctance machines is presented. It starts from the knowledge of machine torque or phase voltages measured at normal operation with AC balanced currents or obtained from dedicated experiments proposed for the BH curve identification. The identification is formulated as an inverse optimization problem where the experimental data based on appropriate experiments serves as the inputs and the BH curve parameters represented with a closed-form expression as the optimization variables. The influence of the different types of measurements on the identified parameters and the optimization process is discussed and compared. Moreover, the impact of geometrical uncertainties due to manufacturing tolerances is investigated and addressed. Virtual measurements obtained form finite-element simulations are used for the study. It is shown that the proposed method can identify the BH curve of the machine core with good accuracy.

Index Terms—**BH curve, Identification, Ferromagntic material, Optimization, Synchronous Reluctance Machines.**

I. Introduction

DSPITE the great progress in the electromagnetic modeling of the electrical machines, it is still a challenging task. Numerical methods like the finite-element (FE) method are powerful and can take account of complex geometries, nonlinearities, and parasitic effects like iron losses and eddy currents [1]. However, owing to uncertainties in the properties of materials, the calculated results of the mathematical models can be different from what is measured in practice.

The magnetic properties of the stator and rotor core have a big effect on the overall performance of the machine [2] [3]. This impact is pronounced particularly in synchronous reluctance (SynRel) machines in which the torque generation solely relies on the difference between direct and quadrature axes inductances [4]. The BH curve of the magnetic steel is usually measured using standard tests and apparatuses like the single sheet tester and Epstein frame [5].

However, the BH curve of the assembled stator and rotor stacks can be different from the one provided by steel manufacturers. The manufacturing process and technology of the electrical machines can degrade the magnetic properties of the steel due to thermal and mechanical residual stress [6]. For example, cutting and shaping the magnetic steel into stator and rotor laminations using punching or laser-cut, welding and compressing the core stack, and stress relief annealing can change the magnetic properties considerably [7], [8].

An alternative approach for the identification of the BH curve is based on measurements obtained from the electromagnetic device itself instead of steel samples. There are several advantages or applications with this approach. It can take account of deterioration of magnetic steel properties due to different manufacturing processes globally, particularly with complex-shaped machine laminations (as opposed to the laminations of a standard Epstein frame). Moreover, sometimes enough information about the device is not available and the

BH curve of the magnetic material needs to be found based on non-invasive methods. In addition, after the prototyping the machine, it may be required to update for example the FE model developed in the design stage for the final design for further studies like force calculation for vibration study.

However, unlike magnetic samples used for standard tests, the flux density inside the elecromagnetic devices, particularly electrical machines, is far from being uniform. Therefore, mapping the relation between the measured data into the material BH curve is challenging. In [9], an optimization-based method for the identification of the BH curve of a ring core, with or without airgap, based on local and global measurements is presented. These measurements are local flux density at different points or the flux linkage of the winding. In [10], a similar method is implemented for the identification of the BH curve of an EI core.

However, measuring local quantities like flux density is not usually possible, particularly in electrical machines, as the magnetic circuit is not readily reachable. In [11], the method is extended to a switched reluctance machine and the BH curve is estimated based on static torque; moreover, the effects of the uncertainty of the airgap length is studied. In [12], the BH curve and hysteresis loop of a ferrite core based on the measurement of the DC and AC inductances for different currents is proposed.

In this paper, an approach for the identification of the BH curve of a SynRel machine is presented. It starts from the knowledge of the phase voltages or torque. The measurements can be obtained with the machine operating at normal condition with AC balanced currents or with DC excitation of the winding while the rotor is externally driven at low speed. Then, the BH curve of the magnetic steel represented by a closed-form relation will be calculated using an optimization inverse problem.

In the next section, the model of the SynRel machine is presented. The effect of the BH curve on the performance of the machine is studied using magnetostatic FE calculations in
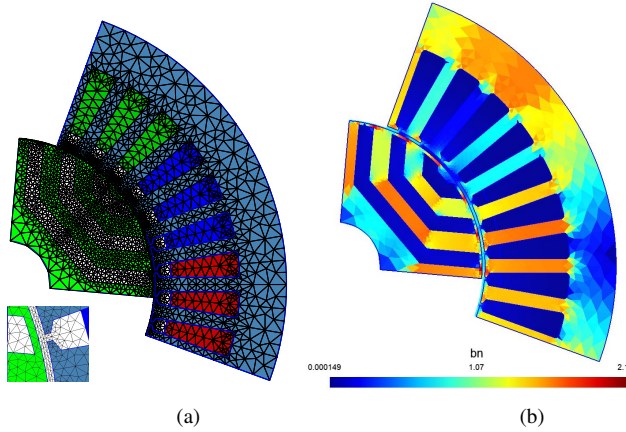
Fig. 1. (a) Cross-section and FE mesh of the SynRel machine and (b) flux density distribution (in T) with $i_\mathrm{d} = i_\mathrm{q} = 6$ A over one pole

TABLE I
SynRel machine parameters

Number of poles	4
Number of slots	36
Stator and rotor lamination	M330-50A
Airgap length (mm)	0.5
Number of turns per coil	30
Fill factor (%)	58
Outer radius of rotor (mm)	25
Outer radius of stator (mm)	48
Stator slot opening (mm)	0.53
Stator tooth width (mm)	2.48
Stator yoke width (mm)	8
Rotor bridge thickness (mm)	0.5
Flux barriers width (mm)	2.5

section III. In section IV, the optimization problem with the torque or phase voltages as the inputs and the parameters of the BH curve as unknowns is formulated. Then, the solution is addressed based on a gradient-based optimization algorithm. The effect of the airgap length uncertainty due to the manufacturing tolerance on the identified BH curve is studied in section V. In section VI, the practical aspects of the proposed method with different types of measurements are discussed. Finally, some conclusions on the proposed method are drawn.

II. The Machine Model

The geometry of the SynRel machine over one pole alongside the mesh used in the following study and an enlarged view of the airgap mesh is shown in Fig. 1 (a). The machine has 2 pole pairs and three slots per phase, per pole. The winding is distributed, full-pitch, and star-connected. The parameters of the machine are reported in Table I.

The model of the machine is implemented using magnetostatic FE method in GetDP/Gmsh. Iron losses and eddy currents are ignored. Moreover, it is assumed that both stator and rotor core are made of the same ferromagnetic material with homogeneous magnetic properties. The flux density distribution with d- and q- axis currents equal to 6A is shown in Fig. 1 (b). It can be seen that the highest flux density occurs in the bridge regions, and flux density in part of flux guide and tooth regions goes up to 2T.

The voltage equations of the machine in dq reference frame are as follows:

$$v_\mathrm{d} = r i_\mathrm{d} + \frac{\mathrm{d}\psi_\mathrm{d}}{\mathrm{d}t} - \omega_\mathrm{r}\psi_\mathrm{q} \tag{1}$$

$$v_\mathrm{q} = r i_\mathrm{q} + \frac{\mathrm{d}\psi_\mathrm{q}}{\mathrm{d}t} + \omega_\mathrm{r}\psi_\mathrm{d} \tag{2}$$

where Ψ_x, i_x, and v_x, with $x \in \{\mathrm{d}, \mathrm{q}\}$, are the d- and q-axis flux linkages, currents, and voltages, respectively. r is the phase resistance, and ω_r the synchronous speed (in electrical rad/s). Since the phase windings are star-connected with isolated neutral point, the zero-sequence components and equation are ignored. Similarly, voltage equations in terms of phase variables can be used; however, in this case, the number of equations increases from two to three. Moreover, the torque is calculated based on Maxwell Stress Tensor using flux density distribution in airgap obtained via FE simulations [13].

III. BH Curve and Sensitivity Analysis

In order to formulate the optimization problem in the next section, the BH curve of the magnetic material needs to be represented using a closed-form relation. There are numerous relations suggested in the literature for both initial AC magnetization curve and hysteresis loops [15]. In this paper, only the AC magnetization curve, simply referred to as BH curve hereafter, is considered. The following relation with three parameters is used for the approximation of the BH curve:

$$B = B_0 \arctan\left(\frac{H}{H_0}\right) + \alpha\mu_0 H \tag{3}$$

where B is flux density in T and H magnetic field in A/m. B_0 in T, H_0 in A/m, and the unitless coefficient α are the three parameters to be identified. However, the proposed method can be utilized with any relation for the BH curve without loss of generality.

The sensitivity of the machine torque and flux linkages to B_0, H_0, and α is investigated. All of the following results are obtained with $i_\mathrm{d} = i_\mathrm{q} = 6$A. Moreover, the reference values of the BH curve parameters are $B_0 = 1.0336$T, $H_0 = 84.3311$A/m, and $\alpha = 1.5000$. These values are obtained based on fitting the BH curve of M330-50A ferromagnetic steel with (3). The original BH curve for M330-50A as well as the fitted BH curve based on (3) are shown in Fig. 2.
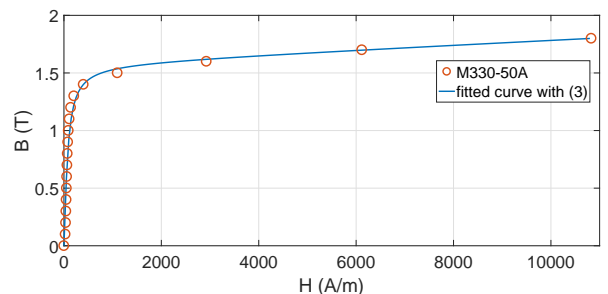

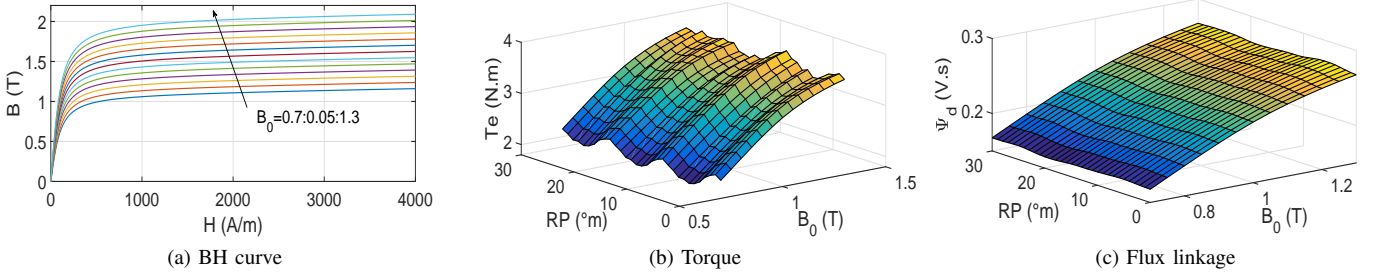Fig. 2. The BH curve of M330-50A [14] alongside the fitted BH curve based on (3)

(a) BH curve

(b) Torque

(c) Flux linkage

Fig. 3. Variation of BH curve, torque, and flux linkage versus B_0 where $B_0 = [0.7 : 0.05 : 1.3]$T with $i_d = i_q = 6$A
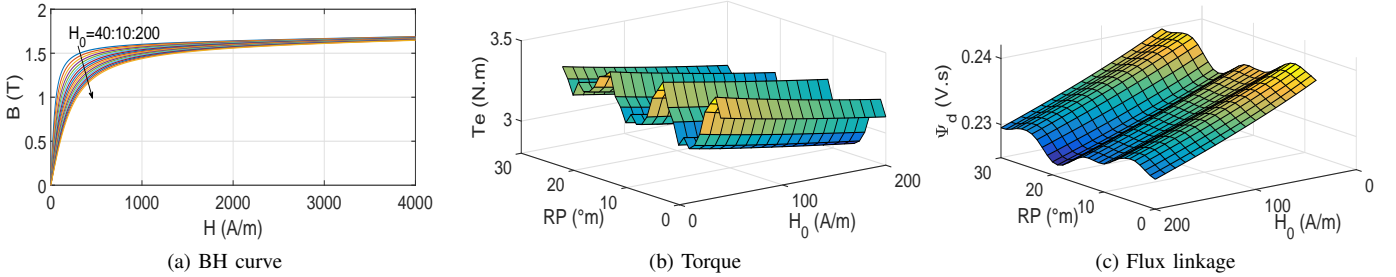

(a) BH curve

(b) Torque

(c) Flux linkage

Fig. 4. Variation of BH curve, torque, and flux linkage versus H_0 where $H_0 = [40 : 10 : 200]$A/m with $i_d = i_q = 6$A

(a) BH curve
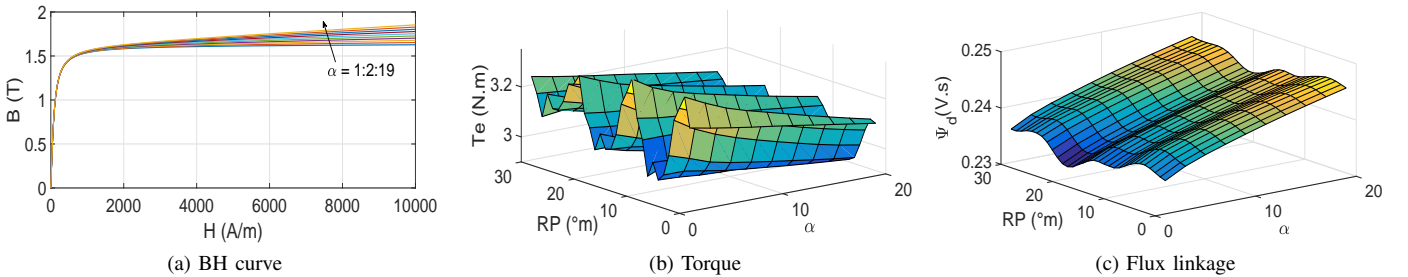
(b) Torque

(c) Flux linkage

Fig. 5. Variation of BH curve, torque, and flux linkage versus α where $\alpha = [1 : 2 : 19]$ with $i_d = i_q = 6$A

In Fig. 3, the variations of the BH curve, the torque, and ψ_d versus B_0 are shown, while B_0 changes from 0.7T to 1.3T with a step of 0.05T. The ψ_q is not shown for the sake of compactness. The B_0 determines the flux density at which the BH curve begins to saturate. The torque and ψ_d are highly sensitive to B_0.

Similarly, in Fig. 4, the variations of the BH curve, the torque, and ψ_d versus H_0 are shown, where H_0 changes from 40 to 200A/m with a step of 10A/m. H_0 mainly affects the field intensity at which the BH curve begins to saturate. The higher H_0 means lower initial permeability of the BH curve. The torque and flux linkage are less sensitive to H_0 compared to B_0. Thus, it may be more challenging to find the "correct" value of this parameter via optimization based on measured values.

Finally, in Fig. 5, similar figures while only α changes from 1 to 19 with a step of 2 are shown. It should be mentioned that the differential permeability should asymptotically convergence to μ_0 at high value of B. Therefore, theoretically α should be equal to 1. However, here it is assumed that the flux density in every point of the stator and rotor core is far below the flux density for which the deferential permeability is close to μ_0. It can be seen unlike the average torque which

TABLE II
OPTIMIZATION PARAMETERS

parameter	Lower limit	Upper limit	initial value
B_0 (T)	0.1	2	0.1
H_0 (A/m)	40	200	40
α	1	20	20

slightly changes, the torque ripple and flux linkage fluctuation are highly sensitive to α.

According to these observations both torque and flux linkage, or corresponding terminal voltage at given currents and speed, are possible measurements which can be used for the identification of B_0, H_0, and α.

IV. IDENTIFICATION OF PARAMETERS

For the identification of the parameters of the BH curve in (3), the optimization problem is defined as follows:

$$\min_{B_0, H_0, \alpha} \frac{1}{N_{\text{sam}}} \sum_{i=1}^{N_{\text{sam}}} \left| \frac{y_{\text{FE},i}(B_0, H_0, \alpha) - y_{\text{sam},i}}{y_{\text{sam},i}} \right| \quad (4)$$

where $y_{\text{sam},i}$ is the ith sample of the measured values, $y_{\text{FE,i}}(B_0, H_0, \alpha)$ the corresponding obtained data using FE model which will be referred to as the calculated values

(a) BH curve

(b) Instantaneous torque with $i_d = i_q = \{2,4,6\}$A
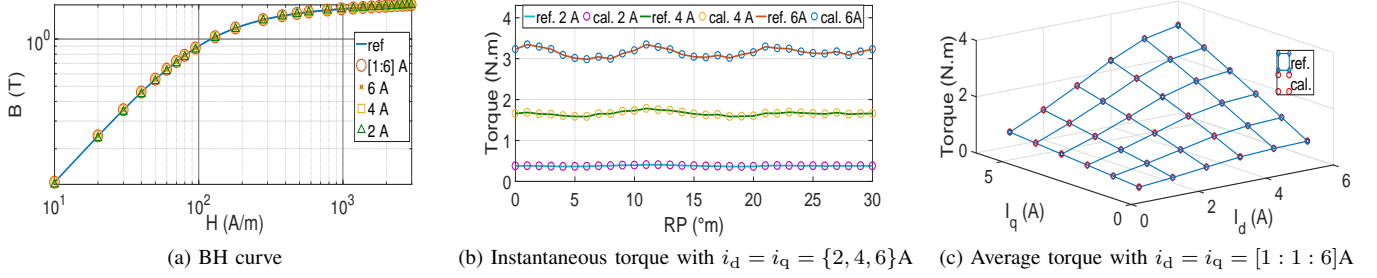
(c) Average torque with $i_d = i_q = [1:1:6]$A

Fig. 6. Calculated BH curve, instantaneous torque, and average torque based on the torque as the reference

(a) BH curve

(b) Instantaneous voltage with $i_d = i_q = \{2,4,6\}$A
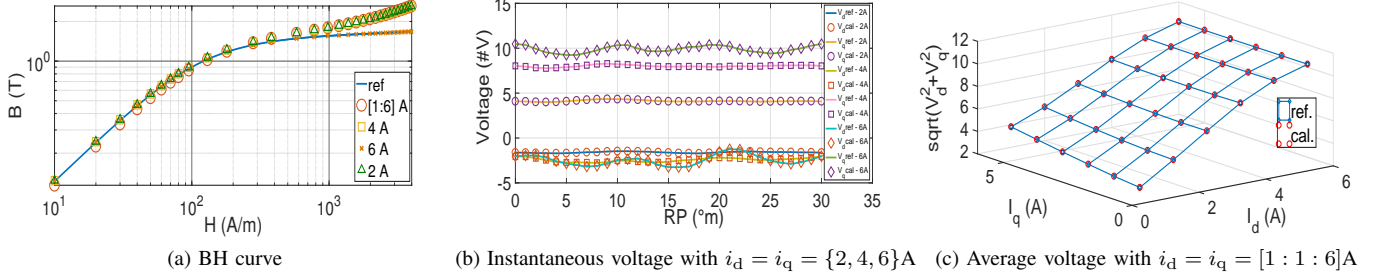
(c) Average voltage with $i_d = i_q = [1:1:6]$A

Fig. 7. Calculated BH curve, instantaneous voltage, and average voltage based on the voltage as the reference

TABLE III
IDENTIFIED PARAMETERS WITH EITHER TORQUE OR VOLTAGE WITH BALANCED CURRENTS AS THE REFERENCE VALUE

		Torque				Voltage			
	ref.	$i_{d,q} = 6$A	$i_{d,q} = 4$A	$i_{d,q} = 2$A	$i_{d,q} = [1:6]$A	$i_{d,q} = 6$A	$i_{d,q} = 4$A	$i_{d,q} = 2$A	$i_{d,q} = [1:6]$A
Iteration	NA	17	18	24	11	13	13	10	9
Fun. value	0	1.5e-06	1.2e-06	7.2e-05	8.1e-07	1.1e-07	3.0e-04	6.7e-05	3.7e-04
B_0 (T)	1.0336	1.0336	1.0336	1.0327	1.0336	1.0336	1.0377	1.0416	1.0439
H_0 (A/m)	84.3311	84.3305	84.3309	86.9294	84.3310	84.3311	85.1592	85.3987	93.1948
α	1.5000	1.5001	1.5007	1.5293	1.5002	1.5000	20.0000	19.9998	20.0000

hereafter, and N_{sam} the number of samples. In this study, the virtual measured data are produced using given values for B_0, H_0, α and will be referred to as the reference values. Then, using the optimization algorithm, the reference values of the BH curve parameters are recovered.

The optimization problem is solved using reflective trust-region method in MATLAB [16]. It is a gradient-based numerical optimization algorithm and compared to stochastic methods like genetic algorithm has higher convergence speed and can give better results for the optimization problem addressed in this paper. Double-sided finite difference is used for the evaluation of the gradients in each iteration. Compared to single-sided finite difference, it gives more accuracy at the cost of higher number of function evaluations and computational effort [16].

The upper and lower limits as well as the initial values of the parameters which are the same in all of the optimizations are reported in Table II. The initial values are selected far away from the reference ones for the investigation of the efficiency of the optimization algorithm in terms of convergence. Moreover, the function tolerance as one of the termination criteria of the algorithm is set to 1e-6. It means that the algorithm will stop iteration when the difference between the last two values of the function is less than the function tolerance. A lower value of the function tolerance obviously leads to lower

error in results. However, it should be adjusted based on the resolution of the measurement equipment. The lower function tolerance means the higher resolution of the measurements.

Two different types of reference values, i.e. torque and voltage "measured" at normal operation with balanced currents and with DC excitation of the windings are used for the identification of the parameters (four different cases in total).

A. Torque with balanced currents

The instantaneous torque over one period is used as the reference value in (4). The sampling rate is $1°$m degree, which amounts to 30 samples over one period. Obviously, a higher number of samples result in less discrepancy between calculated and reference parameters, but it requires higher computational effort. The reference values of parameters for generating the virtual measurements are the same as those in Section III.

The optimization problem is solved for three different current combinations, i.e. $i_d = i_q = \{2,4,6\}$A. The three calculated BH curves along with the reference BH curve are compared in Fig. 6 (a). The corresponding torque profiles versus rotor position (RP) are also shown in Fig. 6 (b). The calculated BH curve parameters, number of iterations, and the objective function values for different current combinations are reported in Table III.
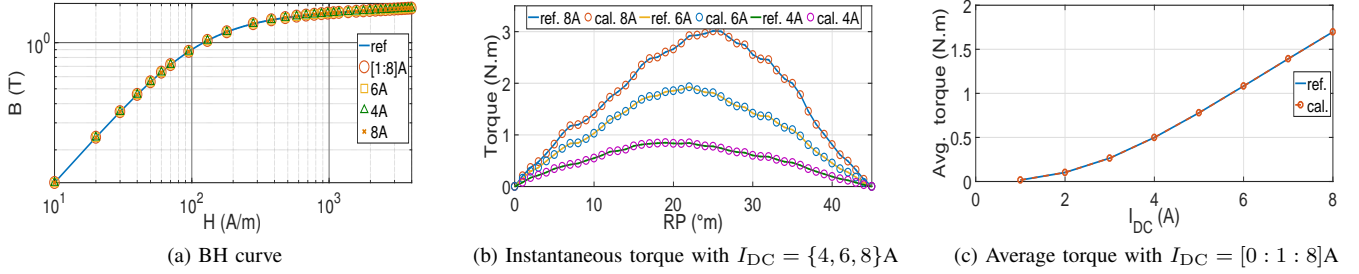
(a) BH curve   (b) Instantaneous torque with $I_{DC} = \{4, 6, 8\}$A   (c) Average torque with $I_{DC} = [0 : 1 : 8]$A

Fig. 8. Calculated BH curve, instantaneous torque, and average torque based on the torque as the reference

(a) BH curve   (b) Instantaneous voltage with $I_{DC} = \{4, 6, 8\}$A   (c) RMS value of induced voltage with $I_{DC} = [0 : 16]$A
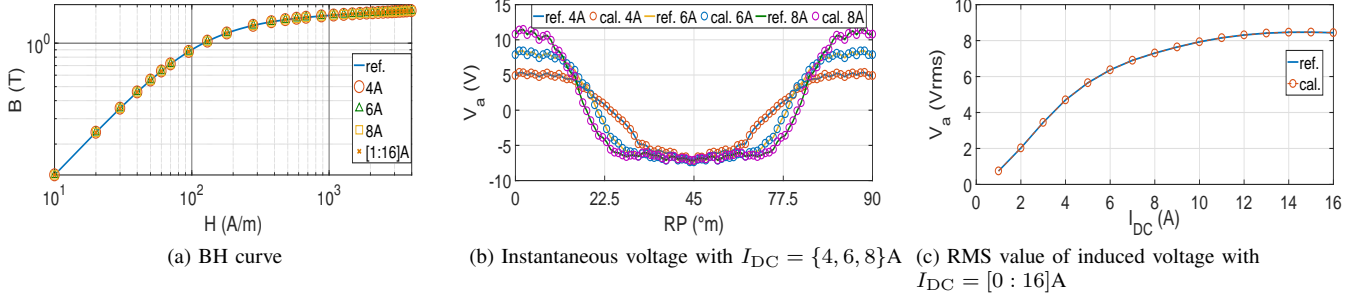
Fig. 9. Calculated BH curve, instantaneous voltage, and average voltage based on the voltage as the reference

There is good agreement between the calculated and reference BH curves and torques for all of current combinations. However, for the higher currents, the agreement is better as the objective function values and number of iterations are lower. It shows that bigger currents which amount to higher saturation lead to more accurate results and it is less challenging for the optimization algorithm to converge to the reference values. It can be attributed to the higher sensitivity of the torque to the BH curve with more saturated core.

Moreover, it can be observed that with different current combinations, the algorithm tries to converge to the reference values, which shows the uniqueness of the inverse problem at least for the selected currents.

Also, the average torque for 36 current combinations, where $i_d = i_q = [1 : 1 : 6]$A, are used as the reference values in (4) and the optimization is carried out again. Compared to the case in which the instantaneous torque over one period is used as the reference value, measuring the average torque is more practical. However, computationally it is more costly to do the optimization for this case, as each function evaluation consists of 36 time-stepping FE runs (the time-stepping run is required for calculating the average torque over one period), compared to one for calculating torque over one period with given currents. The reference and calculated average torque are shown in Fig. 6 (c). Again good agreement is observed.

B. Voltage with balanced currents

Similarly phase voltages can be used as the reference value in (4). With given phase currents and speed, v_d and v_q are calculated using (1) and (2), respectively.

In the same way as torque, the optimization problem for the three different current combinations is solved. Instantaneous values of v_d and v_q are used in (4) simultaneously, which

means 60 samples. Moreover, the average value of v_d and v_q, where $i_d = i_q = [0 : 1 : 6]$ A, is also used as the reference value. All FE simulations are done with constant speed (200 rpm). However, since eddy currents are ignored, the induced voltages change linearly with speed, and therefore the optimization can be done with any non-zero speed.

The calculated parameters of the BH curve as well as the function value and number of iterations are reported in Table III. The calculated BH curves and voltages alongside their reference ones are shown in Fig. 7. It can be seen that with lower currents the identified value of α does not converge to the reference one. Actually, the value of this parameter is the same as the initial value used for the optimization. However, it does not mean that the BH curve depends on the current. The reason is that with lower current values, the flux density in the different parts of the machine is mainly located in the linear region of the BH curve. This region is mainly affected by B_0 and H_0 and not sensitive to α, see Fig. 5 (a). However, with the voltages obtained with $i_d = i_q = 6$A, the agreement between reference and calculated parameters are as good as the case with the torque as reference value.

C. Torque with DC current

In this case phase A and B are paralleled and the winding is supplied with DC current, see Fig. 10 (a). The rotor is rotated using an external mover. Due to magnetic saliency of the rotor, a fluctuating torque with zero average value will be produced.

The torque over one period is used as the reference value in (4). The periodicity of the torque is 90 °m degree. However, as the torque is an odd function of the rotor position, only half of its period is enough for the optimization. The sampling rate is 1 °m degree, and therefore $N_{sam} = 90$. The optimization for three different currents, i.e. $I_{DC} = \{4, 6, 8\}$A, is done.

TABLE IV
IDENTIFIED PARAMETERS WITH EITHER TORQUE OR INDUCED VOLTAGE WITH DC CURRENT AS THE REFERENCE VALUE

	ref.	Torque				Voltage			
		$I_{DC} = 8A$	$I_{DC} = 6A$	$I_{DC} = 4A$	$I_{DC} = [1:8]A$	$I_{DC} = 8A$	$I_{DC} = 6A$	$I_{DC} = 4A$	$I_{DC} = [1:16]A$
Iteration	NA	24	25	25	31	31	27	34	37
Fun. value	0	4.4e-06	1.6e-05	2.3e-06	1e-5	3.4e-06	8.1e-06	4.6e-06	6.0e-05
B_0 (T)	1.0336	1.0336	1.0336	1.0336	1.0336	1.0336	1.0336	1.0336	1.0337
H_0 (A/m)	84.3311	84.3005	84.2075	84.3468	84.2741	84.3337	84.3233	84.3347	84.3313
α	1.5000	1.5079	1.4997	1.4999	1.5078	1.5000	1.5000	1.5000	1.4975

(a) Torque measurement   (b) Induced voltage measurment
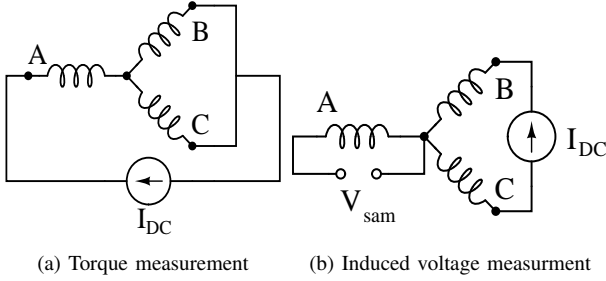
Fig. 10. Winding connection with DC current supply

TABLE V
IDENTIFIED PARAMETERS WITH $i_d = i_q = 6A$ AND WITH/WITHOUT
AIRGAP LENGTH AS AN EXTRA DoF

	ref.	$g_{FE} =$ 0.45 mm	$g_{FE} =$ 0.55 mm	g_{FE} as a DoF
Iteration	NA	23	10	21
Fun. value	0	5.8e-4	15.8e-4	5.7e-05
B_0 (T)	1.0336	1.0392	1.0647	1.0358
H_0 (A/m)	84.3311	191.1298	40.0000	99.9230
α	1.5000	2.2995	1.0646	1.5389
g (mm)	0.5	0.45	0.55	0.494

Moreover, the average of absolute value of torque over one period for different DC currents, where $I_{DC} = [1 : 1 : 8]A$, is used as the reference value as well. In this case, each function evaluation consists of 8 time-stepping FE simulations and $N_{sam} = 8A$.

The reference and calculated BH curves are shown in Fig. 8 (a). Furthermore, the corresponding calculated and reference torques with $I_{DC} = \{4, 6, 8\}A$ and average torque with $I_{DC} = [1 : 1 : 8]A$ are shown in Fig. 8 (b) and (c), respectively. The calculated and reference parameters of the BH curve alongside the number of iterations and function value are reported in Table IV. It can be seen that in this case the identified BH curves are in good agreement with the reference one for all of cases.

D. Induced voltage with DC current

The series connection of B and C are supplied with DC current, while phase A is open-circuited, see Fig. 10 (b). Again thanks to the rotor magnetic saliency, flux due to the currents of phase B and C links with phase A and therefore induces voltage while the rotor is not at standstill. The induced voltage of phase A, V_{sam} (Fig. 10 (b)), is used as the reference value in (4). Unlike the case when torque is the reference value, the rotor speed in this case is important, as V_{sam} is proportional to speed. It is assumed that there is access to the neutral point of the 3-phase winding.

Similarly the optimization with three different currents is done. The periodicity of induced voltage is 90°m degree and $N_{sam} = 90$. Moreover, the RMS value of V_{sam} with $I_{DC} = [1 : 1 : 16]A$ is used as the reference value in (4). As the voltage is less sensitive to the BH curve, higher number of samples with higher currents are used for the measuring the RMS value of the induced voltage.

The calculated and reference BH curves, V_{sam}, and RMS value of V_{sam} are depicted in Fig. 9, respectively. The calculated parameters and the optimization parameters are reported

in Table III. Again it is observed that with low I_{DC} higher number of iterations is required.

V. GEOMETRICAL TOLERANCE

The accuracy of the proposed method depends on how accurate the FE model is. However, in addition to the BH curve of the machine, there are other uncertain parameters. For example, the geometrical dimensions of the machine can vary according to the manufacturing tolerances [17]. If these additional uncertainties are not considered in the FE model, one can expect that the calculated BH curve will deviate from the reference one. However, the additional uncertain parameters can be defined as a degree of freedom (DoF) alongside B_0, H_0, and α.

Among different dimensions, the uncertainty of the airgap length has the biggest impact on the identified BH curve [18]. In order to see the effect of the airgap length on the identified parameters, the airgap length is changed from 0.5 to 0.45mm in the FE model; then, the torque obtained with the airgap 0.5mm and $i_d = i_q = 6A$ is used as the reference value in (4). The same study is done with the airgap length of 0.55mm in the FE model. The calculated parameters are reported in Table IV. The reference and calculated BH curves and torque are shown in Fig. 11. In this case, there is big difference between the reference and calculated parameters.

Alternatively, the airgap length is defined as an optimization variable in (4) and the optimization is repeated with four variables instead of three. The same reference values are used for the optimization and the lower and upper limit of airgap length limit are set to 0.45mm and 0.55mm, respectively. The calculated BH curve is also compared with previous cases in Fig. 11, and the calculated parameters are reported in Table IV. Better agreement between the calculated parameters and the reference ones is observed. Moreover, the identified airgap, 0.494mm, is in good agreement with the original airgap length.
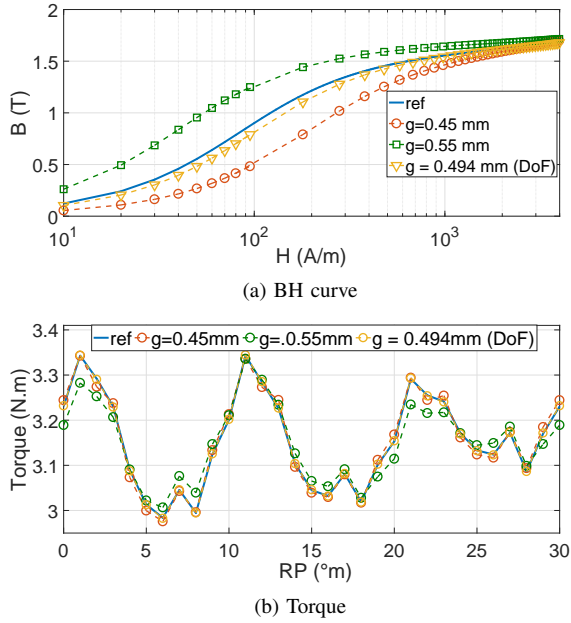
(a) BH curve

(b) Torque

Fig. 11. Calculated values with taking the airgap length effect into account

VI. COMPARISON AND PRACTICAL ASPECTS

The accuracy of the identified parameters strongly depends on the quality of the measurements. The first two methods require the measurement of the torque or voltage in normal operation condition. As the machine needs to be supplied by an inverter, the switching noise can introduce error and reduces the quality of the measurements. Moreover, in the case that the machine is vector controlled, the error of the position sensor also reduces the accuracy of the measurements.

The last two methods need a DC power supply and are more robust against noise. Moreover, the identification based on the average torque or RMS voltage rather than instantaneous values is more favorable in this regard. Large number of experimental data also can reduce the measurement noise.

As torque is more sensitive to the BH curve, it is more suitable for the identification of the BH curve. However, again the measuring of the torque is more challenging than the voltage, as it is more sensitive to the noise and a torque sensor is not always available on the drive system. Moreover, it is necessary to consider the friction torque while measuring the shaft torque of the machine. However, this error due to the friction can be minimized by conducting the tests at standstill or low speeds.

The voltage is not as sensitive as the torque to the BH curve. Therefore, the measurements obtained at high level of saturation is more desirable for the identification. Furthermore, the higher number of measured data with different currents can increase the accuracy of the identified parameters. Moreover, the uncertainty of the phase resistance can introduce error into the measured voltage. In this regard, measuring the induced voltage in one phase while the other two phases are supplied with a DC current is superior. However, it requires access to the neutral point of the winding.

As far as the eddy currents and iron losses are concerned,

the experiments should be conducted at low speed. Ignoring eddy currents and iron loss, the torque is independent of the machine speed, while the induced voltage is proportional to speed. Therefore, the speed should be high enough for measuring voltages with acceptable accuracy given the voltage sensor resolution. Moreover, by adding inertia to the drive, e.g. by mounting a flywheel, the speed fluctuations due to the torque ripple can be minimized and the assumption of constant speed will be more realistic.

Moreover, in this paper it is assumed that the whole core can be represented by a single BH curve. However, in practice the BH curve of some lamination parts with thinner width, like teeth and flux guides in the rotor, may be more deteriorated by the manufacturing process. Moreover, it is possible that the rotor and stator are made of different materials. The proposed method can be extended with several different BH curves for different regions without loss of generality.

VII. CONCLUSION

A method for the magnetic core identification of a SynRel machine was presented which relies on experimental data obtained from the assembled machine. The feasibility of the method was proven via virtual measurements obtained by FE simulations. The measured data can be either torque or voltage while machine is operating with AC balanced currents or excited with DC currents. Compared to the phase voltage, measured torque can result in more accurate results, as it is more sensitive to the BH curve. Moreover, the measurements obtained at higher currents which amounts to higher saturation are more suitable for the BH curve identification. It was shown that geometrical tolerances can strongly affect the accuracy of the identified BH curve. However, such uncertain parameters can be included in the optimization and defined as a DoF besides the BH curve parameters. Provided that the quality measurements are available, the proposed method can successfully be used for the magnetic core identification. However, the method still need to be validated using actual measurements on a real SynRel machine.

REFERENCES

[1] J. Gyselinck and A. C. Pop, "Finite-element and lumped-parameter modelling and simulation of permanent-magnet synchronous machines from academic state of the art to design office practice," in *Tutorial at the International Conference on Electrical Machines (ICEM), Lausanne*, 2016.

[2] S. Rahman, B. Vaseghi, and A. Knight, "Influence of steel BH characteristics on IPMSM performance," in *2012 XXth International Conference on Electrical Machines*. IEEE, 2012, pp. 321–327.

[3] F. Martin, U. Aydin, R. Sundaria, P. Rasilo, A. Belahcen, and A. Arkkio, "Effect of punching the electrical sheets on optimal design of a permanent magnet synchronous motor," *IEEE Transactions on Magnetics*, vol. 54, no. 3, pp. 1–4, 2017.

[4] P. Lazari, K. Atallah, and J. Wang, "Effect of laser cut on the performance of permanent magnet assisted synchronous reluctance machines," *IEEE Transactions on Magnetics*, vol. 51, no. 11, pp. 1–4, 2015.

[5] International Electrotechnical Commission, "Magnetic materials—part 2: Methods of measurement of the magnetic properties of electrical steel sheet and strip by means of an epstein frame," *IEC Standard*, pp. 60 402–2, 1996.

[6] R. Siebert, J. Schneider, and E. Beyer, "Laser cutting and mechanical cutting of electrical steels and its effect on the magnetic properties," *IEEE Transactions on Magnetics*, vol. 50, no. 4, pp. 1–4, 2014.

[7] K. Bourchas, A. Stening, J. Soulard, A. Broddefalk, M. Lindenmo, M. Dahlén, and F. Gyllensten, "Quantifying effects of cutting and welding on magnetic properties of electrical steels," *IEEE Transactions on Industry Applications*, vol. 53, no. 5, pp. 4269–4278, 2017.

[8] O. Perevertov, "Influence of the applied elastic tensile and compressive stress on the hysteresis curves of Fe-3% Si non-oriented steel," *Journal of Magnetism and Magnetic Materials*, vol. 428, pp. 223–228, 2017.

[9] A. Abou-Elyazied Abdallh, P. Sergeant, G. Crevecoeur, L. Vandenbossche, L. Dupré, and M. Sablik, "Magnetic material identification in geometries with non-uniform electromagnetic fields using global and local magnetic measurements," *IEEE Transactions on Magnetics*, vol. 45, no. 10, pp. 4157–4160, 2009.

[10] A. Abou-Elyazied Abdallh, P. Sergeant, G. Crevecoeur, and L. Dupré, "An inverse approach for magnetic material characterization of an ei core electromagnetic inductor," *IEEE Transactions on Magnetics*, vol. 46, no. 2, pp. 622–625, 2010.

[11] A. Abou-Elyazied Abdallh, G. Crevecoeur, and L. Dupré, "A robust inverse approach for magnetic material characterization in electromagnetic devices with minimum influence of the air-gap uncertainty," *IEEE transactions on magnetics*, vol. 47, no. 10, pp. 4364–4367, 2011.

[12] A. Maruo, H. Igarashi, Y. Sato, and K. Kawano, "Identification of magnetization characteristics of material from measured inductance data," *IEEE Transactions on Magnetics*, vol. 55, no. 6, pp. 1–5, 2019.

[13] D. K. Cheng, *Field and wave electromagnetics*. Pearson Education India, 1989.

[14] Cogent Power. [Online]. Available: https://cogent-power.com/products/non-oriented-electrical-steel

[15] Q. Tang, "Investigation of magnetic properties of electrical steel and transformer core at high flux densities," PhD dissertation, The University of Manchester (United Kingdom), 2015.

[16] A. Geletu, "Solving optimization problems using the matlab optimization toolbox-a tutorial," *TU-Ilmenau, Fakultät für Mathematik und Naturwissenschaften*, 2007.

[17] G. Bramerdorfer, "Tolerance analysis for electric machine design optimization: Classification, modeling and evaluation, and example," *IEEE Transactions on Magnetics*, vol. 55, no. 8, pp. 1–9, 2019.

[18] A. Abou-Elyazied Abdallh, G. Crevecoeur, and L. Dupré, "Selection of measurement modality for magnetic material characterization of an electromagnetic device using stochastic uncertainty analysis," *IEEE Transactions on Magnetics*, vol. 47, no. 11, pp. 4564–4573, 2011.